Geophysical Journal International

Geophys. J. Int. (2012) **189,** 1038–1046 doi: 10.1111/j.1365-246X.2012.05406.x

Calculation of normal mode spectra in laterally heterogeneous earth models using an iterative direct solution method

David Al-Attar,[1] John H. Woodhouse[1] and Arwen Deuss[2]

[1] *Department of Earth Sciences, University of Oxford, Oxford* OX1 3PR, *UK. E-mail: david.al-attar@earth.ox.ac.uk*
[2] *Institute of Theoretical Geophysics & Bullard Laboratories, University of Cambridge, Cambridge* CB3 0EZ, *UK*

Accepted 2012 February 1. Received 2012 January 11; in original form 2011 November 25

SUMMARY

Normal mode observations play an important role in studying broad-scale lateral variations in the Earth. Such studies require the calculation of accurate synthetic spectra in realistic earth models, and this remains a computationally challenging problem. Here, we describe a new implementation of the *direct solution method* for calculating normal mode spectra in laterally heterogeneous earth models. In this *iterative direct solution method*, the mode-coupling equations are solved in the frequency-domain using the preconditioned biconjugate gradient algorithm, and the time-domain solution is recovered using a numerical inverse Fourier transform. A number of example calculations are presented to demonstrate the accuracy and efficiency of the method for performing large 'full coupling' calculations as compared to methods based on matrix diagonalization and the traditional direct solution method.

Key words: Surface waves and free oscillations; Seismic tomography; Computational seismology; Theoretical seismology.

1 INTRODUCTION

Normal mode spectra provide a valuable data set for studies of broad-scale lateral variations in the Earth's deep interior (e.g. Woodhouse *et al.* 1986; Giardini *et al.* 1987; Li *et al.* 1991; Resovsky & Ritzwoller 1995, 1998, 1999; He & Tromp 1996; Sharrock & Woodhouse 1998; Deuss 2008; Irving *et al.* 2009; Deuss *et al.* 2010, 2011). In particular, mode spectra are amongst the few geophysical observables that display a non-negligible sensitivity to lateral density variations within the Earth (Ishii & Tromp 1999, 2001; Trampert *et al.* 2004). It is, however, still unclear whether mode data can be used to provide robust estimates of lateral density variations (Romanowicz 2001; Kuo & Romanowicz 2002). Nonetheless, all normal mode studies involve the comparison of observed mode spectra with synthetic spectra calculated in a given laterally heterogeneous earth model. As a result, the calculation of accurate synthetic mode spectra in laterally heterogeneous earth models has long been an important problem in theoretical and computational seismology.

In recent years much progress has been made in the calculation of synthetic seismograms in laterally heterogeneous earth models (e.g. Komatitsch & Tromp 1999, 2002a,b). These advances have been facilitated through both theoretical developments and the continuing increase in available computing power. For the most part, however, the focus of such work has been on modelling relatively high frequency waveforms of interest to body-wave or surface-wave seismology, and the methods developed are not applicable to the calculation of synthetic normal mode spectra. For example, the widely used spectral element method of Komatitsch & Tromp (2002a,b) does not fully incorporate the effects of self-gravitation. As a result, this method cannot accurately model very long period waveforms of interest to normal mode studies. We note that a variation of the spectral element method has been developed by Chaljub & Valette (2004) that does fully incorporate self-gravitation. To our knowledge, however, this method has not been applied to the calculation of mode spectra. More generally, it is not clear that the application of such time-domain fully, numerical methods to normal mode seismology is at present practical due to the great length of the time-series required (tens to hundreds of hours) and the associated computational costs.

All practical methods for computing synthetic normal mode spectra are based upon mode coupling theory that has been developed over many years (e.g. Dahlen 1968, 1969; Woodhouse & Dahlen 1978; Woodhouse 1980, 1983; Woodhouse & Girnius 1982; Park 1986, 1990; Romanowicz 1987; Lognonné & Romanowicz 1990; Tromp & Dahlen 1990; Lognonné 1991; Hara *et al.* 1991, 1993; Um & Dahlen 1992; Deuss & Woodhouse 2004). For a comprehensive review of normal mode seismology see Dahlen & Tromp (1998). Though mode coupling theory is in principle exact, its numerical implementation requires the truncation of the normal mode expansion into a finite set of spherical earth eigenfunctions. Due to computational limitations, early applications of the theory had to employ a number of further approximations, the most common being the so-called *self-coupling* and *group-coupling* approximations in which coupling between only small subsets of the spherical earth eigenfunctions is considered.

Recent work by Deuss & Woodhouse (2001, 2004), Irving *et al.* (2008) and Irving *et al.* (2009) has shown that errors associated

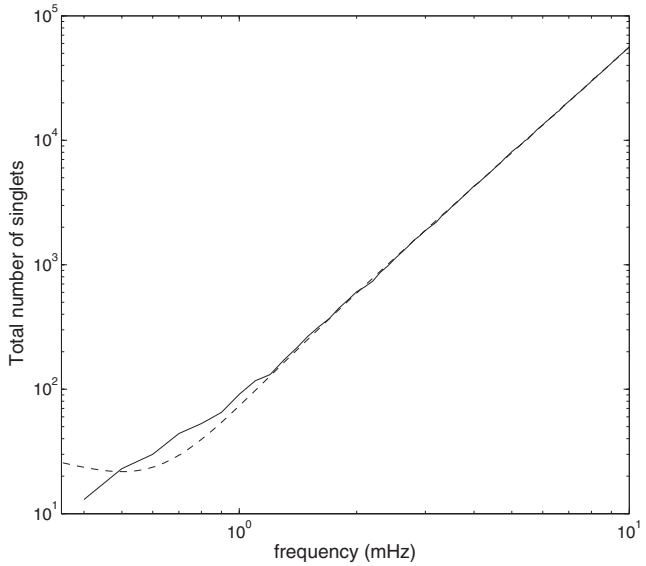

Figure 1. A logarithmic plot (solid line) of the total number of singlet eigenfunctions in PREM (Dziewonski & Anderson 1981) having eigenfrequency less than the frequency specified on the abscissa. The dashed line is the best fitting cubic approximation to this curve.

with the self- and group-coupling approximations can be significant relative to the expected differences between observed and synthetic spectra. Consequently, the use of such approximations in tomographic inversions must cast at least some doubt on the robustness of the earth models obtained. In order to produce sufficiently accurate synthetic spectra it is instead necessary to perform so-called *full-coupling* calculations in which the interaction of large numbers of spherical earth eigenfunctions is taken into account. Such full coupling calculations are likely to be of particular importance in studies of lateral density variations as the effects of density on mode spectra are known to be rather subtle.

The usual method for performing full-coupling calculations is based on diagonalization of the so-called coupling matrix to calculate a subset of the eigenfrequencies and eigenfunctions of the laterally heterogeneous earth model. Once these eigenfrequencies and eigenfunctions are known, synthetic spectra can then be calculated using normal mode summation. This method does, however, suffer from a number of limitations. Most importantly, the computation time for matrix diagonalization rises with the third-power of the dimension of the linear system (Golub & Van Loan 1996). Given that the number of eigenfunctions having eigenfrequency less than a given frequency rises with the third-power of this frequency (see Fig. 1), we see that the computational expense of this method rises approximately with the ninth power of frequency. Moreover, the exact incorporation of rotation into the calculations requires doubling the size of the eigenvalue problem, while linear viscoelasticity can only ever be incorporated in an approximate manner (e.g. Wahr 1981; Deuss & Woodhouse 2001). To circumvent these problems, Deuss & Woodhouse (2004) introduced an iteration method (IM) which provides a numerical method for the calculation of the exact eigenfrequencies and eigenfunctions of a rotating, linear viscoelastic earth model. Moreover, the main computational cost in the IM is the calculation of matrix–vector products with the coupling matrix, and such calculations can readily be parallelized allowing for full-coupling calculations to be performed with very large numbers of coupled modes.

An alternative method for calculating mode spectra is the *direct solution method* (DSM) introduced by Hara *et al.* (1993); see also Dahlen & Tromp (1998) sections 7.7 and 13.3.2 for further discussion of the method. In this approach, the eigenfunctions and eigenfrequencies of the laterally heterogeneous earth model are not calculated. Instead, solutions of the inhomogeneous frequency-domain mode-coupling equations are computed at a range of discrete frequencies to directly produce the synthetic spectra (in detail, such spectra must be processed using discrete Fourier transforms prior to comparison with data obtained from finite-length time-series). The principle advantage of the DSM is that the effects of rotation and linear viscoelasticity can be included in the calculations in an exact and simple manner. Furthermore, with the DSM the calculations at each frequency are independent of one another, and as a result the method can be parallelized in a trivial manner.

In previous implementations of the DSM the inhomogeneous mode coupling equations were solved by performing an LU-decomposition of the coupling matrix followed by back-substitution. The numerical cost of LU-decomposition scales with the third-power of the dimension of the linear system (Golub & Van Loan 1996), so that this approach becomes computationally impractical as the number of coupled modes is increased. In this paper, we describe a new implementation of the DSM that employs an iterative method to solve the inhomogeneous mode coupling equations. This iterative direct solution method (IDSM) does not require the LU-decomposition of the whole coupling matrix, but instead only requires the LU-decomposition of small submatrices and the calculation of matrix–vector products. It is found that computational expense of the DSM scales approximately with the tenth power of the maximum frequency, while that of the IDSM scales with the seventh power of the maximum frequency. As a result, the IDSM offers substantial computational savings over the DSM for performing large full-coupling calculations. The efficiency of the IDSM is also greater than that of methods based on matrix diagonalization for large coupling calculations, particularly due to the fact that the IDSM can be readily parallelized.

2 THEORETICAL BACKGROUND AND METHOD

2.1 Mode coupling equations

By expanding the displacement vector field in terms of the eigenfunctions of a spherically symmetric earth model, the viscoelastodynamic equation in a rotating, laterally heterogeneous, and slightly aspherical earth model can be expressed as an initial value problem for the integro-differential equation

$$\mathbf{P}\partial_t^2\mathbf{u}(t) + \mathbf{W}\partial_t\mathbf{u}(t) + \int_0^t \mathbf{H}(t-t')\mathbf{u}(t')\,\mathrm{d}t' = \mathbf{f}(t), \tag{2.1}$$

subject to the initial conditions

$$\mathbf{u}(0) = \partial_t\mathbf{u}(0) = \mathbf{0}. \tag{2.2}$$

Here $\mathbf{u}$ is a vector containing the expansion coefficients of the displacement vector, $\mathbf{P}$ is the kinetic energy matrix, $\mathbf{W}$ is the Coriolis matrix, $\mathbf{H}(t)$ is the viscoelastodynamic matrix and $\mathbf{f}$ is a vector containing the expansion coefficients of the body-force equivalent of the seismic source. Detailed expressions for these various terms can be found in Woodhouse & Dahlen (1978), Woodhouse (1980), Mochizuki (1986) and Dahlen & Tromp (1998).

We note that expressions for the matrices $\mathbf{P}$, $\mathbf{W}$ and $\mathbf{H}(t)$ given in the above references have been obtained using first-order

perturbation theory to incorporate the effects of aspherical boundaries (internal and external) into the calculations. It is, however, possible to account for such geometric asphericity of the earth model in an essentially exact manner by introducing a mapping from the spherical reference model into the desired aspherical model (see Woodhouse (1978) and Takeuchi (2005) for discussions of closely related problems). Such an approach leads to an equation formally identical to eq. (2.1) though the resulting expressions for the matrices **P, W** and $\mathbf{H}(t)$ differ from those found in the literature, showing an explicit dependence on the mapping from the spherical model into the aspherical model. The numerical implementation of this theory has yet to be carried out in the context of global seismology (Takeuchi (2005) considered a simpler problem in Cartesian geometry), and it remains to be seen whether substantial errors are introduced into mode calculations by the use of boundary perturbation theory.

In principle, the above equation should incorporate coupling of all the eigenfunctions of the spherically symmetric earth model, and so involve infinite-dimensional vectors and matrices. This formulation does, however, exclude the possibility of a continuous component to the normal mode spectrum of the spherically symmetric earth model due to the presence of a non-neutrally stratified fluid outer core (e.g. Rogister & Valette 2008). In practice we can, of course, only deal with finite-dimensional systems of equations, and so we shall suppose that a finite set of eigenfunctions has been chosen for use in the coupling calculations.

2.2 Solution of the mode coupling equations

To solve this equation we shall work in the frequency-domain, using the Fourier-Laplace transform (e.g. Friedlander & Joshi 1998, chapter 10)

$$\tilde{\mathbf{u}}(\omega) = \int_0^\infty \mathbf{u}(t) \mathrm{e}^{-\mathrm{i}\omega t} \, \mathrm{d}t, \tag{2.3}$$

where ω is complex-valued with $\mathrm{Im}(\omega) \leq 0$. For suitably regular functions the inverse Fourier-Laplace transform is given by

$$\mathbf{u}(t) = \frac{1}{2\pi} \int_{-\infty - \mathrm{i}\xi}^{\infty - \mathrm{i}\xi} \tilde{\mathbf{u}}(\omega) \mathrm{e}^{\mathrm{i}\omega t} \, \mathrm{d}\omega, \tag{2.4}$$

where ξ is an arbitrary real number such that all singularities of $\tilde{\mathbf{u}}(\omega)$ lie above the line $\mathrm{Im}(\omega) = -\mathrm{i}\xi$. The transformed version of eq. (2.1) can be written

$$[-\omega^2 \mathbf{P} + \mathrm{i}\omega \mathbf{W} + \tilde{\mathbf{H}}(\omega)] \tilde{\mathbf{u}}(\omega) = \tilde{\mathbf{f}}(\omega), \tag{2.5}$$

where we see that in the frequency-domain viscoelastic effects are manifest through the frequency-dependence of the matrix $\tilde{\mathbf{H}}(\omega)$. This equation can be written more concisely as

$$\tilde{\mathbf{S}}(\omega) \tilde{\mathbf{u}}(\omega) = \tilde{\mathbf{f}}(\omega), \tag{2.6}$$

where we have defined the *coupling matrix* $\tilde{\mathbf{S}}(\omega)$ as

$$\tilde{\mathbf{S}}(\omega) = -\omega^2 \mathbf{P} + \mathrm{i}\omega \mathbf{W} + \tilde{\mathbf{H}}(\omega). \tag{2.7}$$

If, for a given $\omega \in \mathbb{C}$, the matrix $\tilde{\mathbf{S}}(\omega)$ is invertible we define

$$\tilde{\mathbf{G}}(\omega) = \tilde{\mathbf{S}}(\omega)^{-1}, \tag{2.8}$$

and so can write the solution to eq. (2.6) as

$$\tilde{\mathbf{u}}(\omega) = \tilde{\mathbf{G}}(\omega) \tilde{\mathbf{f}}(\omega). \tag{2.9}$$

Values of ω for which $\tilde{\mathbf{S}}(\omega)$ does not have an inverse are eigenfrequencies of the mode coupling equations. We neglect the possibility of gravitation instability of the earth model, in which case it may be shown that all such eigenfrequencies have $\mathrm{Im}(\omega) \geq 0$ (e.g. Dahlen & Tromp 1998, chapter 4). Using the inverse Fourier-Laplace transform, we can write the time-domain solution of the inhomogeneous mode coupling equations as

$$\mathbf{u}(t) = \frac{1}{2\pi} \int_{-\infty - \mathrm{i}\xi}^{\infty - \mathrm{i}\xi} \tilde{\mathbf{G}}(\omega) \tilde{\mathbf{f}}(\omega) \mathrm{e}^{\mathrm{i}\omega t} \, \mathrm{d}\omega, \tag{2.10}$$

where ξ is an arbitrary positive number. Making use of the convolution theorem, this solution can alternatively be written

$$\mathbf{u}(t) = \int_0^t \mathbf{G}(t - t') \mathbf{f}(t') \, \mathrm{d}t', \tag{2.11}$$

where we have defined the time-domain matrix

$$\mathbf{G}(t) = \frac{1}{2\pi} \int_{-\infty - \mathrm{i}\xi}^{\infty - \mathrm{i}\xi} \tilde{\mathbf{G}}(\omega) \mathrm{e}^{\mathrm{i}\omega t} \, \mathrm{d}\omega, \tag{2.12}$$

which may be shown to vanish for negative times. Under certain assumptions it is possible to evaluate the integral in eq. (2.12) to obtain an expression for $\mathbf{G}(t)$ in terms of the eigenvectors of the mode coupling equations. These eigenvectors are non-trivial solutions **u**, say, of the homogeneous frequency-domain mode coupling equations

$$\tilde{\mathbf{S}}(\omega) \mathbf{u} = \mathbf{0}, \tag{2.13}$$

which only exists when ω is an eigenfrequency of the problem (e.g. Dahlen & Tromp 1998; Deuss & Woodhouse 2004; Al-Attar 2007). The eigenvalue problem in eq. (2.13) depends non-linearly on the eigenvalue parameter ω, and so cannot be solved directly using matrix diagonalization. If we neglect viscoelastic effects, eq. (2.13) reduces to a quadratic eigenvalue problem

$$[-\omega^2 \mathbf{P} + \mathrm{i}\omega \mathbf{W} + \mathbf{H}] \mathbf{u} = \mathbf{0}, \tag{2.14}$$

which can be transformed into an eigenvalue problem linear in ω by doubling the size of the system (e.g. Deuss & Woodhouse 2001). Alternatively, we can reduce eq. (2.13) to an eigenvalue problem linear in ω^2 by employing the so-called kinetic and coriolis approximations described by Deuss & Woodhouse (2001). Either of the above two eigenvalue problems can then be solved using standard routines for matrix diagonalization. An important feature of the IM of Deuss & Woodhouse (2004) is that the solution of the non-linear eigenvalue problem in eq. (2.13) can be obtained directly in an exact manner.

An alternative approach to solving the mode coupling equations is the DSM introduced by Hara *et al.* (1993). In this method, solutions of eq. (2.6) are calculated directly at a discrete range of frequencies, and eq. (2.10) is evaluated numerically to obtain the time-domain solution. An attractive feature of the DSM is that rotation and viscoelasticity can be incorporated exactly in a very simple manner and at no extra computational cost. In the previous implementations of the DSM, the linear equations in eq. (2.6) were solved using LU-decomposition of the coupling matrix. The numerical cost of this method rises with the third power of the dimension of the linear system (e.g. Golub & Van Loan 1996), so that its application rapidly becomes unfeasible as the number of coupled modes is increased. In order for the DSM to be applied to large coupling calculations, we shall now describe an iterative method for the solution of the inhomogeneous mode coupling equations.

2.3 Iterative solution of the mode coupling equations

To solve the linear system eq. (2.6) iteratively we make use of the preconditioned biconjugate gradient algorithm (BCG) (e.g. Saad

2000). In this method, an initial guess $\tilde{\mathbf{u}}_0$ for the solution is given, and this solution is iteratively updated until convergence to the actual solution is obtained (here and in the following, we have neglected the dependence of the various terms on ω for notational clarity). The practical choice of an initial solution $\mathbf{u}_0$ is described at the end of this subsection. The efficiency of this method depends crucially on the choice of the preconditioner for the linear system. We recall that a preconditioner for eq. (2.6) is a matrix $\tilde{\mathbf{G}}_0$, say, which is an approximate inverse of $\tilde{\mathbf{S}}$, i.e. we have $\tilde{\mathbf{G}}_0\tilde{\mathbf{S}} \approx \mathbf{1}$. In choosing a suitable preconditioner an important consideration is the trade-off between the effectiveness of the preconditioner and the effort required in its construction (e.g. Chen 2005).

To develop an efficient preconditioner for eq. (2.6) it is useful to consider the structure of the coupling matrix in further detail. It may be shown that $\tilde{\mathbf{S}}$ is partitioned into a number of submatrices, each of which is associated with the coupling of a pair of multiplets of the spherical earth model. The diagonal submatrices represent the effects of self-coupling between multiplets, while the off-diagonal submatrices represent cross-coupling. Moreover, it may be shown that

$$\mathbf{P} = \mathbf{1} + \mathbf{P}^{(1)}, \quad \mathbf{H} = \mathbf{\Omega}^2 + \mathbf{H}^{(1)}, \tag{2.15}$$

where $\mathbf{\Omega}$ is a diagonal matrix whose non-zero entries in each of the self-coupling submatrices are equal to the degenerate eigenfrequency of the associated multiplet. We can, therefore, write

$$\tilde{\mathbf{S}} = (\mathbf{\Omega}^2 - \omega^2\mathbf{1}) + \tilde{\mathbf{S}}^{(1)}, \tag{2.16}$$

where we have defined,

$$\tilde{\mathbf{S}}^{(1)} = -\omega^2\mathbf{P}^{(1)} + \mathrm{i}\omega\mathbf{W} + \mathbf{H}^{(1)}. \tag{2.17}$$

For the frequency-range of interest to seismology, the norm of $\tilde{\mathbf{S}}^{(1)}$ can be shown to be small compared to $|\omega|^2$. It follows that $\tilde{\mathbf{S}}$ is diagonally dominant except within those self-coupling submatrices corresponding to multiplets having eigenfrequencies close to ω. This suggests a preconditioner for eq. (2.6) can be constructed as follows:

(i) Select a frequency bandwidth $\Delta\omega$, and determine which multiplets have eigenfrequencies lying in $(\omega - \Delta\omega, \omega + \Delta\omega)$. Such multiplets are grouped into a *target block*, and remaining multiplets into a *residual block*.

(ii) According to the above decomposition, we write

$$\tilde{\mathbf{S}} = \begin{pmatrix} \left(\mathbf{\Omega}_{11}^2 - \omega^2\mathbf{1}_{11}\right) + \tilde{\mathbf{S}}_{11}^{(1)} & \mathbf{0}_{12} \\ \mathbf{0}_{21} & \left(\mathbf{\Omega}_{22}^2 - \omega^2\mathbf{1}_{22}\right) \end{pmatrix} + \begin{pmatrix} \mathbf{0}_{11} & \tilde{\mathbf{S}}_{12}^{(1)} \\ \tilde{\mathbf{S}}_{21}^{(1)} & \tilde{\mathbf{S}}_{22}^{(1)} \end{pmatrix}, \tag{2.18}$$

where the subscript 11 is used to denote the target block, 22 the residual block, and 12 and 21 the off-diagonal blocks coupling the target and residual blocks. Here the matrices $\mathbf{1}_{11}$ and $\mathbf{1}_{22}$ denote, respectively, the identity-matrices acting on the target and residual blocks, while $\mathbf{0}_{12}$ and $\mathbf{0}_{21}$ are the zero-matrices of the appropriate dimensions.

(iii) The preconditioner for the system is then defined as the inverse of the first of the above matrices

$$\tilde{\mathbf{G}}_0 = \begin{pmatrix} \left\{\left(\mathbf{\Omega}_{11}^2 - \omega^2\mathbf{1}_{11}\right) + \tilde{\mathbf{S}}_{11}^{(1)}\right\}^{-1} & \mathbf{0}_{12} \\ \mathbf{0}_{21} & \left(\mathbf{\Omega}_{22}^2 - \omega^2\mathbf{1}_{22}\right)^{-1} \end{pmatrix}. \tag{2.19}$$

By varying $\Delta\omega$, we can seek a frequency bandwidth which generates an efficient preconditioner. For small values of $\Delta\omega$, the size of the target-block will be small, so that construction of the preconditioner is inexpensive. Such a preconditioner may, however, be a poor approximate inverse of $\tilde{\mathbf{S}}$, so that many iterations may be required for the BCG algorithm to converge. We note that in the extreme case of $\Delta\omega = 0$ the preconditioner is simply the 'spherical earth solution' of the elastodynamic equations. Conversely, for larger values of $\Delta\omega$, the preconditioner will be a better approximate inverse to $\tilde{\mathbf{S}}$ and fewer iterations of the BCG will be required. However, as $\Delta\omega$ is increased the construction of the preconditioner may become prohibitively expensive. Indeed, if $\Delta\omega$ is made sufficiently large, all multiplets will lie in the target-block, and we will simply be using the traditional DSM.

Each iteration of the BCG requires two multiplications of a vector by $\tilde{\mathbf{G}}_0\tilde{\mathbf{S}}$ and one multiplication of a vector by $\tilde{\mathbf{S}}^T\tilde{\mathbf{G}}_0^T$. To perform these matrix–vector multiplications it is not necessary to explicitly construct the preconditioning matrix $\tilde{\mathbf{G}}_0$. To see this, let $\mathbf{v} = \tilde{\mathbf{G}}_0\tilde{\mathbf{S}}\mathbf{w}$ for a given vector $\mathbf{w}$. This relation is equivalent to the linear system $\tilde{\mathbf{G}}_0^{-1}\mathbf{v} = \tilde{\mathbf{S}}\mathbf{w}$, where the matrix $\tilde{\mathbf{G}}_0^{-1}$ is, by definition, equal to

$$\tilde{\mathbf{G}}_0^{-1} = \begin{pmatrix} \left(\mathbf{\Omega}_{11}^2 - \omega^2\mathbf{1}_{11}\right) + \tilde{\mathbf{S}}_{11}^{(1)} & \mathbf{0}_{12} \\ \mathbf{0}_{21} & \mathbf{\Omega}_{22}^2 - \omega^2\mathbf{1}_{22} \end{pmatrix}. \tag{2.20}$$

If we set $\mathbf{z} = \tilde{\mathbf{S}}\mathbf{w}$, and partition $\mathbf{v}$ and $\mathbf{z}$ as

$$\mathbf{v} = \begin{pmatrix} \mathbf{v}_1 \\ \mathbf{v}_2 \end{pmatrix}, \quad \mathbf{z} = \begin{pmatrix} \mathbf{z}_1 \\ \mathbf{z}_2 \end{pmatrix}, \tag{2.21}$$

then the above linear system is equivalent to the two decoupled systems

$$\left\{\left(\mathbf{\Omega}_{11}^2 - \omega^2\mathbf{1}_{11}\right) + \tilde{\mathbf{S}}_{11}^{(1)}\right\}\mathbf{v}_1 = \mathbf{z}_1, \tag{2.22}$$

$$\left(\mathbf{\Omega}_{22}^2 - \omega^2\mathbf{1}_{22}\right)\mathbf{v}_2 = \mathbf{z}_2. \tag{2.23}$$

It follows that we can compute $\mathbf{v} = \tilde{\mathbf{G}}_0\tilde{\mathbf{S}}\mathbf{w}$ by forming one matrix–vector product with $\tilde{\mathbf{S}}$ to compute $\mathbf{z}$, and by solving the above two linear systems for $\mathbf{v}_1$ and $\mathbf{v}_2$. The linear system for $\mathbf{v}_2$ is diagonal, so that its solution may be found trivially. To solve the system for $\mathbf{v}_1$ the LU-decomposition of the matrix $(\mathbf{\Omega}_{11}^2 - \omega^2\mathbf{1}_{11}) + \tilde{\mathbf{S}}_{11}^{(1)}$ is formed, and the solution is then found using back-substitution. A similar argument applies to the calculation of matrix–vector products with $\tilde{\mathbf{S}}^T\tilde{\mathbf{G}}_0^T$. Importantly, the LU-decomposition of the target-block portion of the coupling matrix need only be performed once per frequency.

To proceed practically with the BCG algorithm we must first construct the initial solution $\tilde{\mathbf{u}}_0$. To do this we set

$$\tilde{\mathbf{u}}_0 = \tilde{\mathbf{G}}_0\tilde{\mathbf{f}}, \tag{2.24}$$

where we recall that $\tilde{\mathbf{f}}$ is the given force-vector for the problem. We note that in the case $\Delta\omega = 0$ (so that the target block is empty) this initial solution corresponds to the solution of the equations in the spherical reference model. More generally, for $\Delta\omega = 0$ this initial solution allows some interaction of modes lying within the target block, and so provides a better approximation to the true solution of the problem. Having obtained such a starting value $\tilde{\mathbf{u}}_0$, we then employ the BCG algorithm to construct a sequence of solution vectors $\tilde{\mathbf{u}}_i$ for $i \geq 1$ (see, for example, Saad 2000 for details of the algorithm). At the ith iteration we define the error associated with the solution to be

$$\xi = \frac{\| \tilde{\mathbf{S}}\tilde{\mathbf{u}}_\mathbf{t} - \tilde{\mathbf{f}} \|}{\| \tilde{\mathbf{f}} \|}, \tag{2.25}$$

where $\|\cdot\|$ denotes the standard Hermitian norm of a complex-valued vector, and where we have included the norm $\| \tilde{\mathbf{f}} \|$ of the force-term in the denominator to non-dimensionalize the expression. The BCG algorithm is continued until this error ϵ falls below a certain tolerance value ϵ_0. We have found the choice $\epsilon_0 = 1 \times 10^{-5}$ is sufficient for the resulting spectra obtained using the IDSM to be indistinguishable from those calculated using the DSM for all practical purposes.

3 EXAMPLE CALCULATIONS

In this section, we present a range of calculations to demonstrate the validity and effectiveness of the IDSM. We use spherical earth eigenfunctions calculated in PREM of Dziewonski & Anderson (1981). The laterally heterogeneous earth model used is the S-velocity model S20RTS of Ritsema *et al.* (1999) with perturbations to *P*-wave velocity and density given through the scaling relations

$$\delta v_p/v_p = 0.5\,\delta v_s/v_s, \quad \delta\rho/\rho = 0.3\,\delta v_s/v_s, \tag{3.1}$$

which are suggested by mineral physics (e.g. Karato 1993). In addition to the mantle model, we have incorporated the simple crustal model of Woodhouse & Dziewonski (1984), and include the effects of rotation and elipticity in all calculations. At present we have not implemented viscoelastic attenation exactly within the calculations. Instead, we simply allow the spherical earth eigenfrequencies to have non-zero imaginary parts calculated using first-order perturbation theory. While the exact incorporation of viscoelasticity may have a non-negligible effect on the calculated spectra, it is not thought its presence would alter any of our conclusions about the effectiveness of the IDSM.

3.1 Validation of the iterative method

The accuracy of the IDSM can be most easily verified by comparing its results with those of the traditional DSM. In Fig. 2 such a comparison is shown for a small portion of synthetic spectra, where it is seen that the IDSM rapidly converges to the DSM solution in around three iterations. The rapid convergence of the IDSM seen in this example is found to be typical of the method when applied to full-coupling calculations over the frequency range 0–6 mHz. We note that the upper frequency limit of 6 mHz for these tests has been dictated by the largest size of the coupling matrix that can be stored in memory on the processor used for the calculations (around 13000-by-13000 using single precision complex numbers). Given a processor with larger memory, it is expected that the IDSM would be similarly effective for higher frequency full coupling calculations. In particular, by using parallel computing it would be possible to distribute the coupling matrix between the memories of a large number of processors, and in this manner consider the full-coupling of very large numbers of modes.

To further verify the efficacy of the IDSM, we have extensively benchmarked the method against existing codes for solving the mode coupling equations using matrix diagonalization. As expected, it is found that the results of the IDSM agree to numerical precision with those of matrix-diagonalization so long as rotation is incorporated exactly into these latter calculations by doubling the size of the eigenvalue problem. In Fig. 3 is shown an example of the errors associated with the kinetic and Coriolis approximations that are commonly used in the matrix diagonalization method to incorporate lateral density variations and rotation without doubling the size of the eigenvalue problem. Though these errors are relatively

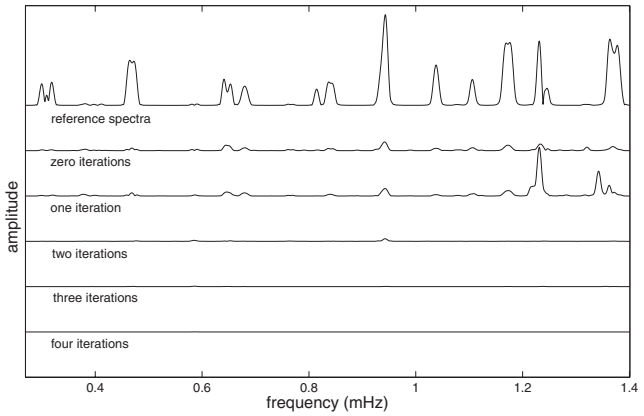

Figure 2. In the uppermost trace is plotted a portion of synthetic vertical acceleration amplitude spectra at the station AFI for the 1994 June 9, Bolivia earthquake that has been calculated using the DSM coupling all modes having eigenfrequency less than 3 mHz (giving a total of 1883 coupled singlets). For this calculation a 96 hr time-series was generated to which a cosine-bell window in the range 5–65 hr was applied prior to determination of the amplitude spectra. The lower five traces plot the difference between this reference spectra and the spectra produced using the stated number of iterations of the IDSM. Note that the 'difference' we have plotted is equal the modulus of the difference between the two complex spectra, and so reflects misfit in both amplitude and phase. For these calculations the chosen frequency-bandwidth $\Delta f = \frac{1}{2\pi}\Delta\omega$ used in the IDSM was 0.05 mHz. It is seen from this figure that the IDSM is able to rapidly converge to the exact solution of the mode coupling equations.

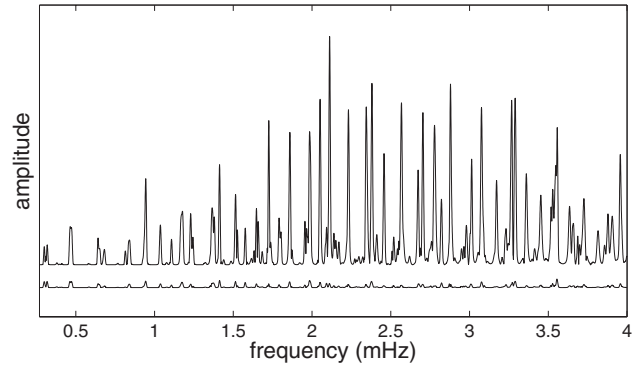

Figure 3. In the uppermost trace is plotted a portion of synthetic vertical acceleration amplitude spectra at the station AFI for the 1994 June 9, Bolivia earthquake that has been calculated using the IDSM coupling all modes having eigenfrequency less than 4.3 mHz (giving a total of 5190 coupled singlets). For this calculation a 96 hr time-series was generated to which a cosine-bell window in the range 5–65 hr was applied prior to determination of the amplitude spectra. In the lower trace is plotted the difference between this reference spectra and the result of performing the same calculation but now employing the Coriolis and kinetic approximations of Deuss & Woodhouse (2001).

small, it is obviously preferable to use a method that does not necessitate such approximations, and an attractive feature of the DSM and IDSM is that both lateral density variations and rotation can be taken into account exactly at no extra computational expense.

3.2 Choice of $\Delta\omega$ for the target-block

The efficiency of the preconditioner used in the IDSM depends on the choice of the frequency bandwidth $\Delta\omega$ used for the target block. In Fig. 4 we plot the variation with $\Delta f = \frac{1}{2\pi}\Delta\omega$ in (a) total calculation time, (b) mean number of iterations for convergence,

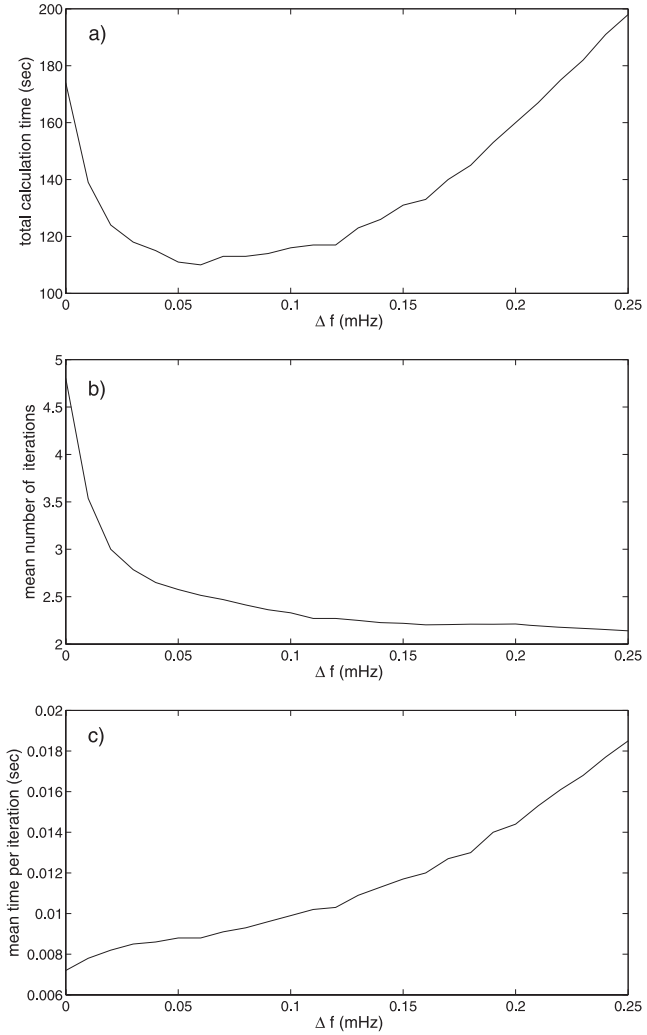

Figure 4. Variation in (a) total calculation time, (b) mean number of iterations per frequency, and (c) mean calculation time per iteration , with choice of the frequency bandwidth parameter $\Delta f = \frac{1}{2\pi}\Delta\omega$. For these calculations all modes with eigenfrequencies less than 2 mHz are included, and a 96 hr time-series is generated.

and (c) mean calculation time per iteration. It is seen that as $\Delta\omega$ increases the number of iterations needed for convergence of the BCG algorithm decreases monotonically; this is because as $\Delta\omega$ increases the preconditioner $\tilde{\mathbf{G}}_0$ becomes a closer approximation to $\tilde{\mathbf{S}}^{-1}$. However, as $\Delta\omega$ is increased more work must be done to construct the preconditioner, and it is seen that the mean time per iteration increases correspondingly. In Fig. 4 (a) it is seen that due to these opposing effects, the total calculation time initially decreases with increasing $\Delta\omega$, reaches a minimum at around $\Delta f \approx 0.05$ mHz, and then starts to rise again. The precise value of this minimum depends on the details of the calculation (such as number of modes coupled, and length of the time-series), though the choice $\Delta f \approx 0.05$ mHz seems, in general, to work well.

3.3 Comparison of the IDSM and DSM

To demonstrate the advantage of the IDSM over the DSM, it is useful to investigate how the calculation time required by the two methods scales with the maximum frequency of the coupled modes. To do this we computed synthetic spectra using the two methods coupling all modes having eigenfrequencies less than a given value

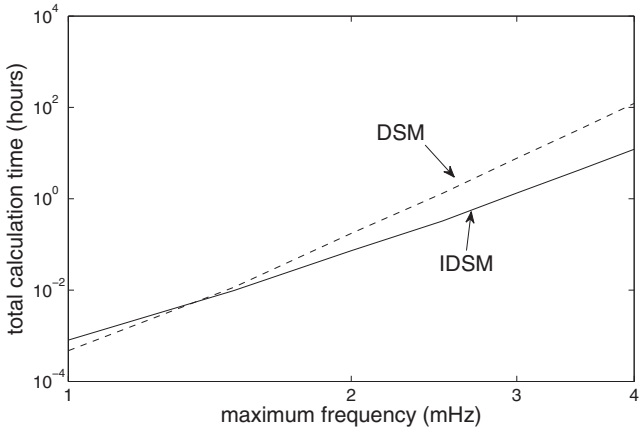

Figure 5. Comparison of the mean calculation time per frequency between the traditional DSM and the IDSM as the maximum frequency of coupled modes is increased. Examination of the slopes of these two plots shows that for the DMS the total calculation timescales roughly like the tenth power of the maximum frequency, while for the IDSM the scaling is with the seventh power of the maximum frequency.

$f_{\max}$ for $f_{\max} = 1$ through to 4.0 mHz in 0.5 mHz intervals. In each calculation the length of the time-series produced was 96 hr, and the number of frequency steps was chosen based on this time to achieve good spectral resolution. The results of these calculations are summarized in Fig. 5 where we plot the total calculation time against the maximum frequency $f_{\max}$ on logarithmic axes. From the gradients of the corresponding plots it is seen that the total calculation for the DSM scales roughly like tenth power of $f_{\max}$, while for the IDSM the scaling is with the seventh power of $f_{\max}$. We note that the calculations for these figures were performed on a single processor, and that the calculation times for both the DSM and IDSM can be substantially reduced in practice by performing the calculations for different frequencies in parallel.

These results can be seen to be consistent with theoretical expectations as follows. For both problems the size of the linear system scales with $f_{\max}^3$ (see Fig. 1), and the total number of frequencies at which the mode coupling equations are solved scales like $f_{\max}$. In the DSM the most expensive computational step is the LU-decomposition of the coupling matrix which scales with the third power of the dimension of the linear system, and so we would expect the total calculation time for the DSM to scale like $f_{\max}^{10}$. For the IDSM the most expensive computational step is the calculation of matrix–vector products which scale with the second power of the linear system, and so we would expect the total calculation time for the IDSM to scale like $f_{\max}^7$. Because of this difference in scaling between the two methods, it is clear that for large coupling calculations the IDSM is significantly more effective than the DSM.

3.4 Effects of truncating the coupling equations

In setting up the mode coupling equations we must select a finite subset of spherical earth multiplets we wish to consider. This truncation of the infinite-dimensional mode coupling equations necessarily introduces an error into the calculations. An important question therefore arises: suppose we wish to calculate synthetic spectra in a given frequency range (ω_1, ω_2), then which multiplets must be included in the coupling calculations in order for the resulting spectra to be sufficiently accurate? By 'sufficiently accurate' here we mean, roughly speaking, that the difference between calculated spectra and

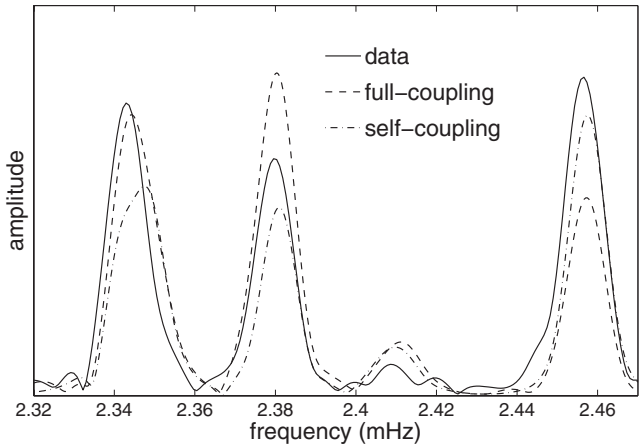

Figure 6. Vertical acceleration amplitude spectra at the station AFI for the 1994 June 9 Bolivia earthquake. The solid line shows the data amplitude spectra obtained from the observed time-series by deconvolving the instrument response and applying a cosine-bell window in the range 5–65 hr prior to calculation of the discrete Fourier transform. The amplitude spectra labelled 'full-coupling' and 'self-coupling' are synthetics for the event calculated with the IDSM in the laterally heterogeneous model S20RTS (Ritsema *et al.* 1999) using scaling relations given in eq. (3.1) for perturbations in *P*-wave speed and density. For the 'full-coupling' calculation the coupling of all modes having eigenfrequency less than 4.3 mHz is considered, while for the 'self-coupling' calculation only coupling between modes lying in the same spherical earth multiplet is allowed. It is apparent that for this portion of spectra the errors associated with the self-coupling approximation are of the same order of magnitude as the difference between the observed data and calculated synthetics.

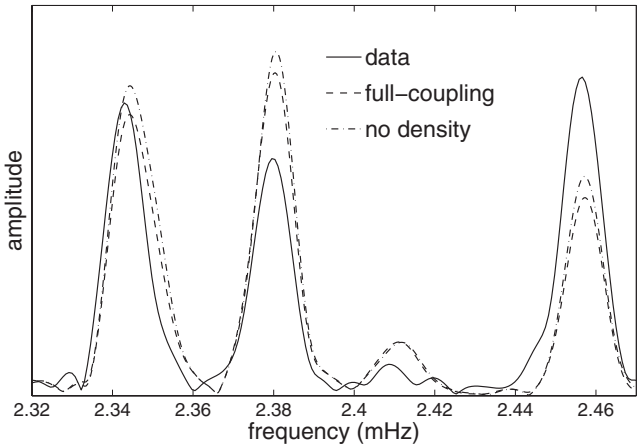

Figure 7. As for Fig. 6 except here the amplitude spectra labelled 'no density' is a synthetic for the event calculated using full-coupling of all modes having eigenfrequency less than 4.3 mHz but for which the density perturbation in the laterally heterogeneous earth model is set equal to zero. Comparison with the 'self-coupling' spectra of Fig. 6 shows that for this portion of spectra the errors associated with self-coupling approximation are larger than the likely effects of lateral density variations in the Earth.

the exact spectra are smaller than the expected differences between synthetic and observed spectra for the real Earth.

In early normal mode studies the choice of which modes to include in coupling calculations was largely motivated by computational expediency. In particular, it was usual to employ the self-coupling approximation in which only coupling between modes lying in the same spherical earth multiplet is allowed. This approximation greatly reduced the computational demands of normal mode calculations, and also led naturally to the introduction of splitting functions (Giardini *et al.* 1987) which remain an important tool for studying the Earth's interior (Deuss *et al.* 2011). However, the self-coupling approximation provides, at best, a rather crude solution of the mode coupling equations, and recent work by Deuss & Woodhouse (2001, 2004), Irving *et al.* (2008), and Irving *et al.* (2009) has highlighted the need to move towards full-coupling calculations. The importance of full-coupling calculations is likely particularly pronounced in studies of lateral density variations within the Earth as the excepted effects of such density variations on observed spectra are likely quite subtle.

In Fig. 6 we plot a portion of observed amplitude spectra at the station AFI for the June 9 Bolivia earthquake. Also plotted in this figure are two synthetic spectra calculated in the laterally heterogeneous earth model S20RTS (Ritsema *et al.* 1999) using the IDSM. The synthetic spectra labelled 'full-coupling' was calculated by allowing coupling between all modes having eigenfrequencies less than 4.3 mHz, while the spectra labelled 'self-coupling' was calculated using the self-coupling approximation. The upper frequency limit used in the 'full-coupling' calculation was chosen so that no appreciable change in the plotted spectra occurred when additional higher frequency modes were included in the calculation. As a result, the 'full-coupling' spectra can be used as an exact reference spectra against which the accuracy of other methods can be assessed. For the portion of spectra plotted in Fig. 6, it is seen that the errors associated with the self-coupling approximation are of the same order of magnitude as the difference between observed spectra and reference synthetic calculated in a good laterally heterogeneous earth model. Furthermore, in Fig. 7 we have plotted the same observed spectra and 'full-coupling' synthetic as in Fig. 6, but have now included a synthetic spectra labelled 'no density' that has been calculated in the same way as the 'full-coupling' synthetic except that the laterally density perturbation in the earth model is set equal to zero. Taking the difference between the 'full-coupling' and 'no density' spectra to be indicative of the expected 'order-of-magnitude' changes due to lateral density variations, we see from comparison of Figs 6 and 7 that for this portion of spectra the errors associated with the self-coupling approximation are in fact significantly larger than the effects of density on the spectra.

Errors associated with the self-coupling approximation over a wider range of frequencies can be seen in Fig. 8. Here the uppermost trace labelled 'full-coupling' is a synthetic amplitude spectra at the station AFI for the 1994 Bolivia earthquake calculated using the IDSM in S20RTS (Ritsema *et al.* 1999) using the P-velocity and density scalings described in eq. (3.1). The trace labelled 'no density' shows the difference between this reference spectra and that calculated in the same manner but with the density perturbation set equal to zero (note the plotted difference is the modulus of the difference between the two complex spectra, and so contains information about both amplitude and phase). The trace labelled 'self-coupling' plots the difference between the reference 'full-coupling' spectra and a synthetic spectra in S20RTS with non-zero density perturbations but calculated using the self-coupling approximation. Comparison of the 'no density' and 'self-coupling' traces shows that over the whole of the frequency range 04 mHz the errors associated with the self-coupling approximation are comparable in magnitude, and in fact generally larger, than the effects of lateral density variations on the spectra.

An intermediate step between the self-coupling approximation and full-coupling is the so-called group-coupling approximation in

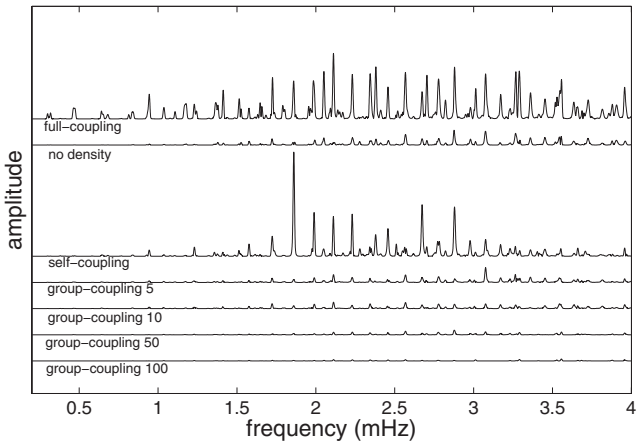

Figure 8. In the uppermost trace is plotted a portion of synthetic vertical acceleration amplitude spectra at the station AFI for the 1994 June 9 Bolivia earthquake. This reference 'full-coupling' spectra has been calculated for S20RTS (Ritsema *et al.* 1999) employing the scaling relations in eq. (3.1) for *P*-velocity and density perturbations using the IDSM coupling all modes having eigenfrequency less than 4.3 mHz. For this calculation a 96 hr time-series was generated to which a cosine-bell window in the range 5–65 hr was applied prior to determination of the amplitude spectra. The trace labelled 'no density' shows the difference between the reference 'full-coupling' spectra and that calculated using the same number of coupled modes but with the density perturbation in the model set equal to zero. The remaining five traces show the difference between the reference 'full-coupling' spectra and those calculated in S20RTS including the non-zero density perturbation but using either the self-coupling or group-coupling approximations. For group-coupling calculations we allowed coupling between the stated number of nearest neighbour multiplets (see the main text for further details).

which coupling between the modes lying in a relative small group of spherical earth multiplets is considered. In Fig. 8 we also examine the errors associated with a particular form of group-coupling. To do this we have ordered all the multiplets used in the 'full-coupling' calculation in terms of their eigenfrequencies. We then specified a 'nearest-neighbour' coupling width n, and allowed coupling of the modes lying in each spherical earth multiplet with those lying in the nearest n neighbouring spherical earth multiplets. We note that if $n > 0$ this form of group coupling does allow some indirect coupling between all modes considered. From Fig. 8 it is seen that even with $n = 50$ the errors associated with group-coupling are not negligible compared to the effects of density. These calculations again highlight the potential shortcomings of commonly used approximate methods for performing normal mode calculations, and reiterate the need for allowing coupling of large numbers of multiplets in order to calculate very accurate synthetic mode spectra.

The results of the example calculations shown in Figs 6, 7 and 8 constitute prima facie evidence that the self- and group-coupling approximations may not be sufficiently accurate for studies of lateral variations in Earth structure, and, in particular, for studies of lateral density variations. The situation is, however, somewhat more complicated. The applicability of these approximations depends strongly on the modes being studied, and also on the processing done to the time-series in order to produce the spectra. As a result, practical studies employing the self- and group-coupling approximations carefully select which modes to examine, and apply appropriate time-windows and filters to the observed data so as to lessen the influence of coupling with unwanted modes. To rigorously assess the applicability of these approximations to studies of Earth structure it is, therefore, necessary to consider specific modes of interest, and to incorporate the effects of any processing done to the data. Moreover, such an investigation into the resolvability of a given model parameter cannot simply rely on the comparison by eye of a few synthetic spectra. Instead, the relevant question to ask – for definiteness, in the context of splitting function studies using the self-coupling approximation – is the extent to which the splitting function obtained agrees with the self-coupling part of the generalized splitting function determined through the full-coupling of all modes. If the self-coupling splitting function measurements are found to be robust in the above sense, then inferences about Earth structure based upon them will be similarly robust.

4 DISCUSSION

In this paper, we have described a new iterative implementation of the direct solution method for the calculation of synthetic seismograms in laterally heterogeneous earth models. Numerical tests show that this method is significantly more efficient than the traditional DSM for performing large coupling calculations. The IDSM provides a useful alternative to matrix-diagonalization methods for performing full coupling calculations, and offers the advantage that both rotation and viscoelascity can be incorporated exactly at essentially no extra computational expense. At present the number of coupled modes considered in our calculations is limited by the memory available on a single processor. The IDSM is, however, well suited to implementation on parallel computers on which very large coupling matrices may be distributed between the memories of the different processors.

As a first application of the method, we have conducted a preliminary investigation of the importance of full-coupling calculations for studies of lateral density variations within the Earth. We have shown that the likely effects of lateral density variations on observed spectra can be of the same order of magnitude as the errors that are associated with the self- or group-coupling approximations. As a result, it is not clear whether these approximations are sufficiently accurate for use in inversions of lateral density variations from normal mode spectra. This conclusion is, however, rather tentative, and we feel that this issue bears further and detailed investigation.

ACKNOWLEDGMENTS

DA-A is supported through a Junior Research Fellowship at Merton College, Oxford. AD has been funded by the European Research Council under the European Community's Seventh Framework Programme (FP7/2007–2013)/ERC grant agreement 204995 and a Leverhulme Prize. We thank two anonymous reviewers for their detailed comments that have greatly helped in the preparation of this work.

REFERENCES

Al Attar, D., 2007. A solution of the elastodynamic equation in an anelastic earth model, *Geophys. J. Int.,* **170,** 755–760.

Chaljub, E. & Valette, B., 2004. Spectral-element modeling of three-dimensional wave propagation in a self-gravitating Earth with an arbitrarily stratified outer core, *Geophys. J. Int.,* **158,** 131–141.

Chen, K., 2005. *Matrix Preconditioning Techniques and Applications,* Cambridge University Press, Cambridge.

Dahlen, F.A., 1968. The normal modes of a rotating, elliptical earth, *Geophys. J. R. astr. Soc.,* **16,** 329–367.

Dahlen, F.A., 1969. The normal modes of a rotating, elliptical earth—near-resonance multiplet coupling, *Geophys. J. R. astr. Soc.,* **18,** 397–436.

Dahlen, F.A. & Tromp, J., 1998. *Theoretical Global Seismology,* Princeton University Press, Princeton, NJ.

Deuss, A., 2008. Normal mode constraints on shear and compressional wave velocity of the Earth's inner core, *Earth planet. Sci. Lett.,* **268,** 364–375.

Deuss, A., Irving, J.C.E. & Woodhouse, J.H., 2010. Regional variations of inner core anisotropy from seismic normal mode observations, *Science,* **328,** 1018–1020.

Deuss, A., Ritsema, J. & van Heijst, H., 2011. Splitting function measurements for Earth's longest period normal modes using recent large earthquakes, *Geophys. Res. Lett.,* **38,** L04303, doi:10.1029/2010GL046115.

Deuss, A. & Woodhouse, J.H., 2001. Theoretical free-oscillation spectra: the importance of wide band coupling, *Geophys. J. Int.,* **146,** 833–842.

Deuss, A. & Woodhouse, J.H., 2004. Iteration method to determine the eigenvalues and eigenvectors of a target multiplet including full mode coupling, *Geophys. J. Int.,* **159,** 326–332.

Dziewonski, A. & Anderson, D.L., 1981. Preliminary reference Earth model, *Phys. Earth planet. Int.,* **25,** 297–356.

Friedlander, G. & Joshi, M., 1998. *Introduction to the Theory of Distributions,* Cambridge University Press, Cambridge.

Giardini, D., Li, X-D. & Woodhouse, J.H., 1987. Three dimensional structure of the Earth from splitting in free oscillation spectra, *Nature,* **325,** 405–411.

Golub, G.H. & Van Loan, C.F, 1996. *Matrix Computations,* The John Hopkins University Press, Baltimore, MD.

Hara, T., Tsuboi, S. & Geller, R.J., 1991. Inversion for laterally heterogeneous earth structure using a laterally heterogeneous starting model: preliminary results, *Geophys. J. Int.,* **104,** 523–540.

Hara, T., Tsuboi, S. & Geller, R.J., 1993. Inversion for laterally heterogeneous upper mantle S-wave velocity structure using iterative waveform inversion, *Geophys. J. Int.,* **115,** 667–698.

He, X. & Tromp, J., 1996. Normal-mode constraints on the structure of the earth, *J. geophys. Res.,* **101,** 20053–20082.

Irving, J.C.E., Deuss, A. & Andrews, J., 2008. Wide band coupling of Earth's normal modes due to anisotropic inner core structure, *Geophys. J. Int.,* **174,** 919–975.

Irving, J.C.E., Deuss, A. & Woodhouse, J.H., 2009. Normal mode coupling due to hemispherical anisotropic structure in Earth's inner core, *Geophys. J. Int.,* **178,** 962–975.

Ishii, M. & Tromp, J., 1999. Normal-mode and free-air gravity constraints on lateral variations in velocity and density of the Earth's mantle, *Science,* **285,** 1231–1236.

Ishii, M. & Tromp, J., 2001. Even-degree lateral variations in the Earth's mantle constrained by free oscillations and the free-air gravity anomaly, *Geophys. J. Int.,* **145,** 77–96.

Karato, S., 1993. Importance of anelasticity in the interpretation of seismic tomography, *Geophys. Res. Lett.,* **20,** 1623–1626.

Komatitsch, D. & Tromp, J., 1999. Introduction to the spectral element method for three-dimensional seismic wave propagation, *Geophys. J. Int.,* **139,** 806–822.

Komatitsch, D. & Tromp, J., 2002a. Spectral-element simulations of global seismic wave propagation—I. Validation. *Geophys. J. Int.,* **149,** 390–412.

Komatitsch, D. & Tromp, J., 2002b. Spectral-element simulations of global seismic wave propagation—II. 3-D models, oceans, rotation, and self-gravitation, *Geophys. J. Int.,* **150,** 303–318.

Kuo, C. & Romanowicz, B., 2002. On the resolution of density anomalies in the Earth's mantle using spectral fitting of normal mode data, *Geophys. J. Int.,* **150,** 162–179.

Li, X.-D., Giardini, D. & Woodhouse, J.H., 1991. Large scale three dimensional even degree structure of the earth from splitting of long period normal modes, *J. geophys. Res.,* **96,** 551–577.

Longnonné, P., 1991. Normal modes and seismograms in an anelastic rotating earth, *J. geophys. Res.,* **96,** 20 309–20 319.

Lognonné, P. & Romanowicz, B., 1990. Modelling of coupled normal modes of the Earth: the spectral method, *Geophys. J. Int.,* **102,** 365–395.

Mochzuki, E., 1986. The free oscillations of an anisotropic and heterogeneous Earth, *Geophys. J. Int.,* **86,** 167–176.

Park, J., 1986. Synthetic seismograms from coupled free oscillations: effects of lateral structure and rotation, *J. geophys. Res.,* **91**(B6), 6441–6464.

Park, J., 1990. The subspace projection method for constructing coupled-mode synthetic seismograms, *Geophys. J. Int.,* **101,** 111–123.

Resovsky, J.S. & Ritzwoller, M.W., 1995. Constraining odd-degree earth structure with coupled free-oscillations. *Geophys. Res. Let.,* **22,** 2301–2304.

Resovsky, J.S. & Ritzwoller, M.W., 1998. New and refined constraints on three-dimensional earth structure from normal modes below 3 mHz, *J. geophys. Res.,* **103,** 783–810.

Resovsky, J.S. & Ritzwoller, M.W., 1999. A degree 8 shear velocity model from normal mode observations below 3 mHz, *J. geophys. Res.,* **104,** 993–1014.

Ritsema, J., van Heijst, H.J. & Woodhouse, J.H, 1999. Complex shear wave velocity structure imaged beneath Africa and Iceland, *Science,* **286**(5446), 1925–1928.

Rogister, Y. & Valette, B., 2008. Influence of liquid core dynamics on rotational modes, *Geophys. J. Int.,* **176,** 368–388.

Romanowicz, B., 1987. Multiplet-multiplet coupling due to lateral heterogeneity: asymptotic effects on the amplitude and frequency of the earth's normal modes, *Geophys. J. R. astr. Soc.,* **90,** 75–100.

Romanowicz, B., 2001. Can we resolve 3D density heterogeneity in the lower mantle?, *Geophys. Res. Let.,* **28,** 1107–1110.

Saad, Y., 2000. *Iterative Methods for Sparse Linear Systems,* 2nd edn, SIAM, Philadelphia, PA.

Sharrock, D.S. & Woodhouse, J.H., 1998. Investigation of time dependent inner core structure by analysis of free oscillation spectra, *Earth Planets Space,* **50,** 1013–1018.

Trampert, J., Deschamps, F., Resovsky, J. & Yuen, D., 2004. Probabilistic tomography maps chemical heterogeneities throughout the lower mantle, *Science,* **306,** 853–856.

Tromp, J. & Dahlen, F.A., 1990. Free oscillations of a spherical anelastic earth, *Geophys. J. Int.,* **103,** 707–723.

Um, J. & Dahlen, F.A., 1991. Normal mode multiplet coupling along a dispersion branch, *Geophys. J. Int.,* **106,** 11–35.

Wahr, J.M., 1981. A normal mode expansion for the forced response of a rotating earth, *Geophs. J. R. astr. Soc.,* **64,** 651–675.

Woodhouse, J.H., 1980. The coupling and attenuation of nearly resonant multiplets in the Earth's free oscillation spectrum, *Geophys. J. R. astr. Soc.,* **61,** 261–283.

Woodhouse, J.H., 1983. The joint inversion of seismic waveforms for lateral variations in earth structure and earthquake source parameters, in *Proc. Enrico Fermi Int. Sch. Phys,* Vol. LXXXV, pp. 366–397, eds Kanamori, H. & Boschi, E., Societa Italiana di Fisica, Italy.

Woodhouse, J.H. & Dahlen, F.A., 1978. The effect of a general aspherical perturbation on the free oscillations of the earth, *Geophys. J. R. astr. Soc.,* **53,** 335–354.

Woodhouse, J.H. & Dziewonski, A., 1984. Mapping the Upper Mantle: three-dimensional modeling of Earth structure by inversion of seismic waveforms. *J. geophys. Res.,* **89,** 5953–5986.

Woodhouse, J.H. & Girnius, T.P., 1982. Surface waves and free oscillations in a regionalized earth model. *Geophys. J. R. astr. Soc.,* **68,** 653–673.

Woodhouse, J.H., Giardini, D. & Li, X.D., 1986. Evidence for inner core anisotropy from free oscillations, *Geophys. Res. Lett.,* **13,** 1549–1552.